Molecular Therapy
Oncology
Original Article

Bortezomib promotes the TRAIL-mediated killing of resistant rhabdomyosarcoma by ErbB2/Her2-targeted CAR-NK-92 cells via DR5 upregulation

Catrin Heim,[1,8] Leonie Hartig,[1,8] Nadine Weinelt,[2] Laura M. Moser,[1,3,4,5,8] Emilia Salzmann-Manrique,[1,8] Michael Merker,[1,5,8] Winfried S. Wels,[3,4,6] Torsten Tonn,[7] Peter Bader,[1,5,8] Jan-Henning Klusmann,[3,4,5,8] Sjoerd J.L. van Wijk,[2,3,5] and Eva Rettinger[1,3,4,5]

[1]Goethe University Frankfurt, Department of Pediatrics, Division of Stem Cell Transplantation and Immunology, 60590 Frankfurt am Main, Germany; [2]Institute for Experimental Paediatric Haematology and Oncology (EPOH), 60528 Frankfurt am Main, Germany; [3]German Cancer Consortium (DKTK), partner site Frankfurt am Main, a partnership between DKFZ and University Hospital and Georg-Speyer-Haus, Frankfurt am Main, Germany; [4]Frankfurt Cancer Institute (FCI), 60596 Frankfurt am Main, Germany; [5]Universitäres Centrum für Tumorerkrankungen (UCT) Frankfurt Marburg, 60590 Frankfurt am Main, Germany; [6]Georg-Speyer-Haus, Institute for Tumor Biology and Experimental Therapy, 60596 Frankfurt am Main, Germany; [7]DRK-Blutspendedienst Baden-Württemberg/Hessen gemeinnützige GmbH, 60505 Frankfurt am Main, Germany; [8]Goethe University Frankfurt, Department of Pediatrics, 60590 Frankfurt am Main, Germany

Treatment resistance and immune escape are hallmarks of metastatic rhabdomyosarcoma (RMS), underscoring the urgent medical need for therapeutic agents against this disease entity as a key challenge in pediatric oncology. Chimeric antigen receptor (CAR)-based immunotherapies, such as the ErbB2 (Her2)-CAR-engineered natural killer (NK) cell line NK-92/5.28.z, provide antitumor cytotoxicity primarily through CAR-mediated cytotoxic granule release and thereafter—even in cases with low surface antigen expression or tumor escape—by triggering intrinsic NK cell-mediated apoptosis induction via additional ligand/receptors. In this study, we showed that bortezomib increased susceptibility toward apoptosis in clinically relevant RMS cell lines RH30 and RH41, and patient-derived RMS tumor organoid RMS335, by upregulation of the tumor necrosis factor-related apoptosis-inducing ligand (TRAIL) receptor DR5 in these metastatic, relapsed/refractory (r/r) RMS tumors. Subsequent administration of NK-92/5.28.z cells significantly enhanced antitumor activity *in vitro*. Applying recombinant TRAIL instead of NK-92/5.28.z cells confirmed that the synergistic antitumor effects of the combination treatment were mediated via TRAIL. Western blot analyses indicated that the combination treatment with bortezomib and NK-92/5.28.z cells increased apoptosis by interacting with the nuclear factor κB, JNK, and caspase pathways. Overall, bortezomib pretreatment can sensitize r/r RMS tumors to CAR- and, by upregulating DR5, TRAIL-mediated cytotoxicity of NK-92/5.28.z cells.

INTRODUCTION

Rhabdomyosarcoma (RMS) is the most common pediatric soft tissue sarcoma, with an annual incidence of 4.5 cases per million in children, adolescents, and young adults.[1] RMS can be subdivided into two histological subtypes, embryonal and alveolar (aRMS), and scored clinically. Risk stratification follows standard protocols (e.g., from the Children's Oncology Group or the European Pediatric Soft Tissue Sarcoma Study Group). Patients of any age who have tumors at any site and of any size with lymph node involvement and suffer from fusion-driven (*PAX3/7-FOXO1*) aRMS (subgroup G) or patients with metastatic disease (subgroup H) are scored as "very high risk" for treatment failure. The majority of patients with relapsed/refractory (r/r) RMS succumb to their disease within a median time span of 2 years with conventional therapies, emphasizing the urgent unmet medical need for novel treatment strategies.[2,3]

Chimeric antigen receptor (CAR)-carrying immune effector cells can be highly effective as a treatment, even in cases with low surface antigen expression.[4] We and others have identified ErbB2 (Her2) as a suitable target for CAR-based immunotherapy of RMS.[5] In the context of RMS, the ErbB2-CAR-engineered natural killer (NK) cell line NK-92/5.28.z showed excellent cytotoxicity in preclinical *in vitro* and *in vivo* analyses.[6] Upon binding of a CAR to a target antigen on the cell surface, cancer cell apoptosis is mainly triggered by the release of the contents of cytotoxic granules, including granzyme A/B and perforin, into the synaptic cleft between the effector and target cells. After primary degranulation of NK-92/5.28.z cells, apoptosis is also induced by cell-death-inducing ligands such as Fas ligand or tumor necrosis factor-related apoptosis-inducing ligand (TRAIL). In parallel, the secretion of interferon-γ (IFN-γ) increases the expression of major histocompatibility complex class II on tumor cells, thereby leading to an immune-enriched tumor microenvironment (TME).[7,8] However, while most

Received 18 August 2023; accepted 8 April 2024;
https://doi.org/10.1016/j.omton.2024.200802.

Correspondence: Eva Rettinger, Goethe University Frankfurt, Department of Pediatrics, Division of Stem Cell Transplantation, Immunology and Intensive Care Medicine, 60590 Frankfurt am Main, Germany.
E-mail: eva.rettinger@icloud.com

RMS cancers are resistant to conventional immune- and Fas-mediated cytotoxicity of T cells, susceptibility toward TRAIL and target engagement with tumor-specific CARs might be faced by NK-92/5.28.z cells.[9] The limited life span of NK-92/5.28.z cells resulting in treatment failure *in vivo*[10] might be additionally addressed, i.e., by combination with other anticancer therapies that increase the susceptibility of r/r RMS tumors to TRAIL-mediated cytotoxicity of NK-92/5.28.z cells and bystander cells within the TME, such as bortezomib.

Bortezomib, also known as PS-341, is a dipeptidyl boronic acid that selectively and reversibly inhibits the 26S proteasome.[11] Bortezomib, the first proteasome inhibitor tested in humans, showed a favorable safety profile and potent antitumor activity, particularly in patients with refractory or progressive multiple myeloma (MM).[12] Bortezomib was approved by the US Food and Drug Administration in 2003 under the trade name Velcade for the treatment of MM. Inhibition of the 26S proteasome, an essential multiprotein complex required for protein degradation, leads to apoptosis. Stabilization of tumor suppressors p21, p27, and p53, as well as proapoptotic proteins Bid, Bax, and Noxa, and the prevention of nuclear factor κB (NF-κB) signaling are considered key factors for bortezomib-mediated apoptosis.[13–15] In a multicenter phase 2 study investigating bortezomib as a single agent for the treatment of metastatic sarcoma, the inhibitor was well tolerated but showed limited efficacy,[16] suggesting combination treatment, e.g., via TRAIL, as proteasomal inhibition leads to overexpression of TRAIL receptors (TRAIL-Rs) on the surfaces of various cancer types.[17,18]

TRAIL-mediated apoptosis is mediated by both NK and cytotoxic T cells.[19] TRAIL expression on the surfaces of immune cells leads to trimerization of TRAIL-R molecules on the surfaces of cancer cells, leading to recruitment of the Fas-associated death domain (FADD) and activation of pro-caspase-8 through autocleavage of caspase-8 to induce apoptosis by activating caspase-3.[20,21] TRAIL-resistant cancer cells, including hepatoblastoma, glioblastoma, and pancreatic cancer cell lines, can be sensitized to TRAIL-induced apoptosis by pretreatment with bortezomib.[22,23] In cases of renal carcinoma, pretreatment with bortezomib prior to CAR-NK-92 cell therapy led to significantly reduced amount of tumor growth compared to single-agent therapy in a preclinical *in vivo* model.[24] Whether bortezomib also increases the susceptibility of RMS tumors to bortezomib-mediated apoptosis and/or TRAIL-mediated killing via NK-92/.28.z cells is not yet known.

In this study, we investigated the effects of proteasome inhibition by bortezomib and the combination treatment of bortezomib and CAR-NK-92 cells redirected against ErbB2 in defined *in vitro* models of ErbB2-expressing, r/r, and, in part, TRAIL-resistant aRMS tumors.

RESULTS

aRMS cells are sensitive to bortezomib treatment

The anticancer effects of the proteasome inhibitor bortezomib were assessed in the clinically relevant aRMS cell lines RH30 and RH41, as well as in the patient-derived aRMS tumor organoid cell line RMS335, representing metastatic, r/r RMS tumors.[25,26] The RH30 cell line was established from a xenograft of bone marrow obtained from a 16-year-old male with untreated metastatic aRMS. The RH41 cell line was established from a xenograft of a lung metastasis from 7-year-old female patient following treatment for aRMS.[26] RMS tumoroid model RMS335 was established from a lymph node metastasis of a 7-year-old female patient with a second relapse of aRMS.[25]

RH30 cells were used as a reference to determine the appropriate incubation time for experiments with aRMS cells. aRMS cells were transduced with luciferase before being used in luciferase-based toxicity assays.[27] Cytotoxic effects of bortezomib treatment were quantified based on dose-response curves. At 24 and 48 h (Figures 1A and 1B), dose-response curves reached a plateau. After 48 h, curves showed a steep ascent and therefore a low half-maximal effective concentration (EC_{50}) value of 2.1 nM. Therefore, incubation periods of 24 h were used for further experiments. aRMS cells showed sensitivity toward bortezomib treatment and EC_{50} values of 29.6 nM for RH30 (Figure 1A), 23.7 nM for RH41 (Figure 1C), and 6.1 nM for RMS335 cells (Figure 1D), indicating increased susceptibility of the tumor organoid cells toward apoptosis but no final execution of apoptosis in cancer cells by treatment with bortezomib.

Caspase cleavage and caspase-3/7 activation upon bortezomib treatment

Western blot analysis of RH30 (Figure 2A, left) and RH41 cells (Figure 2A, right) was performed to assess caspase-3 cleavage upon bortezomib treatment. Caspase-3 was cleaved into 17 kDa fragments upon the treatment of RH30 and RH41 cells with 25 and 10 nM bortezomib, respectively. Cleavage-mediated caspase activation was further assessed by Caspase-Glo assays. The RH30 (Figure 2B) and RH41 (Figure 2C) cell lines accordingly showed significant activation of caspase-3/7 after bortezomib treatment (25 nM), whereas no significant activation effects of caspase-3/7 were observed in the RMS335 tumor organoid cell line by Caspase-Glo assays (Figure 2D).

Enhanced surface expression of TRAIL-R DR5, but not DR4, after bortezomib treatment

Bortezomib can enhance the surface expression of TRAIL-Rs DR4 and DR5 on various cell types and thereby sensitizes these cells to TRAIL-mediated apoptosis of T or NK cells.[28–30] The surface expression levels of the TRAIL-Rs DR4 and DR5 on aRMS cells, assessed by flow cytometry analysis after treatment with 0, 5, 10, 25, or 50 nM bortezomib for 24 h, are shown in Figure 3. While DR4 was not expressed, DR5 surface expression was upregulated in a dose-dependent manner in all analyzed aRMS cells after 24 h pretreatment with bortezomib.

Bortezomib pretreatment enhances the lysis of aRMS cells by NK-92/5.28.z cells

NK-92/5.28.z cell-mediated killing is mainly executed via cytotoxic granule release and granzyme B expression, followed by expression of death ligands such as TRAIL and TRAIL-mediated killing via the

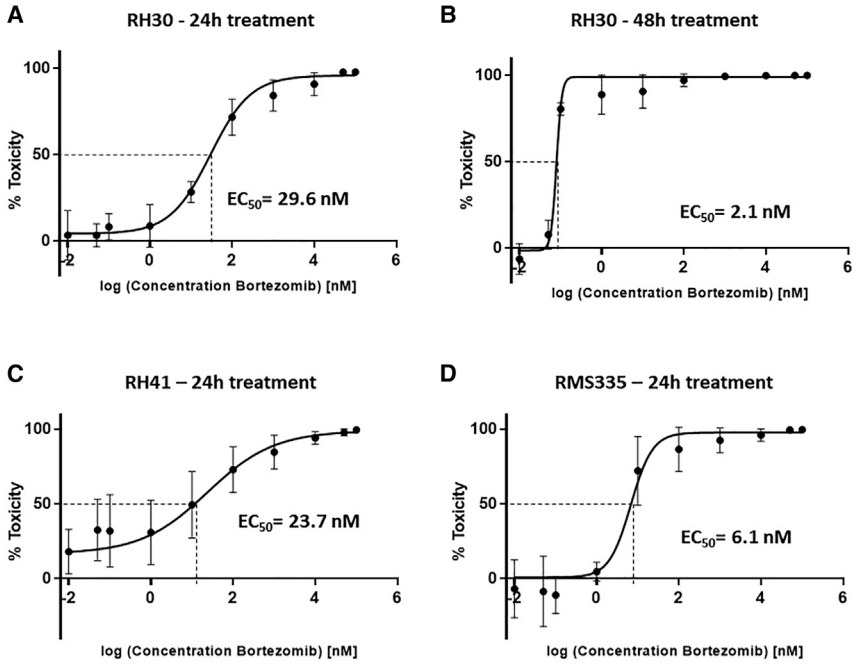

Figure 1. Determination of EC_{50} values of the aRMS cell lines RH30 and RH41 and the tumor organoid aRMS RMS335 in the presence of increasing bortezomib doses, shown using the luciferase toxicity assays

(A and B) Luciferase-expressing RH30 cells were incubated for 24 h (A) and 48 h (B) with the indicated concentrations of bortezomib. After 24 and 48 h, luciferase was added to bortezomib-pretreated target cells and untreated controls. Cell lysis was calculated based on the luminescence signals of remaining cells and correlated with the signal of the untreated controls. (C and D) The EC_{50} values of RH41 (C) and RMS335 (D) were determined analogously after 24 h of treatment with the indicated bortezomib concentrations. The results of at least three independent experiments are shown. After 24 h incubation, the dose-response curve showed a corresponding effect on the RMS cells with EC_{50} values (dotted lines) in the nanomolar range.

caspase cascade. Bortezomib pretreatment upregulated expression of the TRAIL-R DR5, allowing for potentially enhanced TRAIL-mediated killing by NK-92/5.28.z cells. Indeed, significantly increased cytotoxicity was observed against RH30 (Figure 4A), RH41 (Figure 4B), and RMS335 cells (Figure 4C) after bortezomib pretreatment. However, susceptibility toward NK-92/5.28.z cell cytotoxicity was not exclusively related to surface TRAIL expression on target cells. Nevertheless, our data indicate significantly enhanced lysis of aRMS cells by NK-92/5.28.z cells after pretreatment with bortezomib, even at nanomolar concentrations.

Effects of combination treatment on aRMS cell lines

Activation of the NF-κB pathway, one of the main pathways of innate and adaptive immune functions that serves as a pivotal mediator of inflammatory responses,[31] is highly dependent on the proteasomal degradation machinery. The *in vitro* effects of bortezomib on the NF-κB pathway in RMS remain unclear. Therefore, activation of the NF-κB pathway was assessed by quantifying mRNA expression levels by quantitative polymerase chain reaction (qPCR) (Figures 5A, RH30, and 5B, RH41) and/or protein phosphorylation levels by western blot analysis (Figure 5C, RH30 on the left and RH41 on the right) in aRMS cells after combination treatment with NK-92/5.28.z cells and bortezomib. Significantly enhanced p100 mRNA levels were detected in RH30 and RH41 aRMS cell lines after NK-92/5.28.z cell treatment, while protein levels remained stable. Especially in RH30 cells, increased p100 phosphorylation was detected after NK-92/5.28.z cell treatment. p65 expression remained stable upon treatment. Furthermore, the phosphorylation level of p65 was not affected by combination treatment or single-agent therapy in either aRMS cell line. B-cell lymphoma-extra large (BCL-xL) mRNA and protein levels did not change upon combination treatment or single-agent treatment. Notably, low Bcl-xL protein expression was detected in RH41 cells. In contrast, c-Jun N-terminal kinase (JNK) mRNA levels significantly decreased after NK-92/5.28.z cell or combination treatment, but not after single-agent bortezomib treatment, in RH30 cells. Notably, single-agent NK-92/5.28.z cells and combination treatment resulted in the cleavage of caspase-3 in both RH30 and the TRAIL-resistant RH41 cells.

Bortezomib synergizes with TRAIL-induced apoptosis

As the cytotoxicity of NK-92/5.28.z cells is at least partially mediated by TRAIL, its contribution to the overall cytotoxicity of the combination treatment was evaluated. To avoid additional cytotoxic influences through NK-92/5.28.z cells, purified TRAIL protein was used for cytotoxicity analysis. Cytotoxicity data were analyzed with the zero interaction potency (ZIP) model (Figure 6) to uncover potential synergistic effects between TRAIL and bortezomib. The ZIP reference for additive cytotoxic effects (top boxes) for RH30 (Figure 6A), RH41 (Figure 6B), and RMS335 cells (Figure 6C) showed TRAIL sensitivity of RH30 and TRAIL resistance of RH41 and RMS335 cells. The ZIP synergy score was calculated by comparing the observed combined effect of bortezomib and TRIAL versus the expected individual effects. The observed combined effect of bortezomib and TRIAL was increased in comparison to the sum of the monotherapies resulting in a positive score, which indicated synergetic interaction between bortezomib and TRIAL. Hence, the experimental data modeled by the ZIP synergy score model (bottom boxes) showed significant synergistic effects for the combination treatment against RH30 (p = 1.43e−5) and RMS335 (p = 4.58e−3) and a tendency of synergism against RH41 cells (p = 1.90e−1).

DISCUSSION

For metastatic and r/r RMS, the responses to conventional therapies, such as local therapies and systemic chemotherapy, are not long-lasting in most cases.[32] Recently, the use of novel ErbB2-CAR-T cell

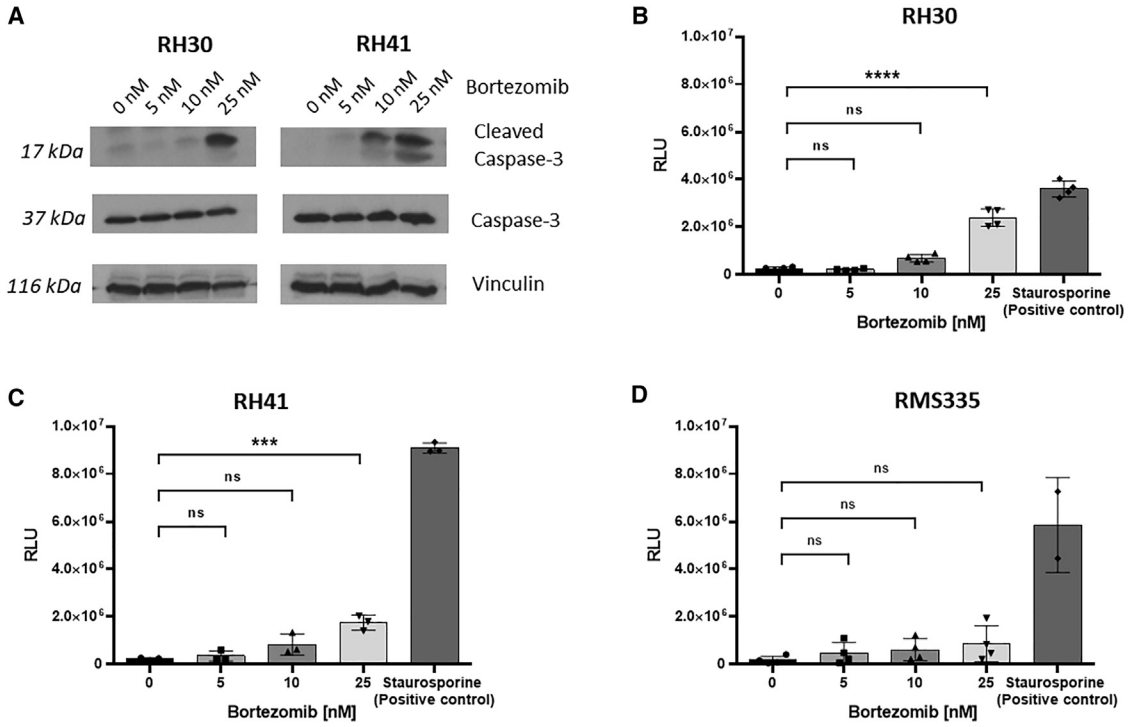

Figure 2. Caspase-3 cleavage and caspase-3/-7 activity in aRMS target cells after bortezomib treatment

aRMS cells were treated with different concentrations of bortezomib. (A) After 24 h, aRMS cells were lysed and caspase cleavage was assessed by western blot analysis: RH30 (left) and RH41(right). In addition to caspase cleavage, caspase activation was determined by Caspase-Glo assay. (B–D) For this purpose, RH30 (B), RH41 (C) and RMS335 (D) cells were treated with the indicated bortezomib concentrations for 24 h, and caspase-3/7 activity was quantified using a Caspase-Glo assay according to the manufacturer's instructions. Caspase-3 was cleaved and activated in RH30 and RH41 cells but not in RMS335 cells. The results are presented as the mean ± standard deviation (SD), and one-way ANOVA with the Bonferroni method was used to evaluate differences. Differences for $^{*}p < 0.05$, $^{**}p < 0.01$, $^{***}p < 0.005$, and $^{****}p < 0.001$ were considered significant.

therapy in combination with checkpoint inhibition demonstrated aRMS sensitivity to immune cell cytotoxicity, which supports the use of cellular immunotherapy to evoke anti-RMS immunity in general.[33] However, intrinsic features such as low target antigen expression,[6,34] low mutational burden, and thus low neoantigen content as well as the immunosuppressive TME[35–37] have impeded the development of cellular immunotherapy for aRMS.

ErbB2 has been shown to be a valid and promising target for CAR engineering in RMS by Hegde et al.[33] The ErbB2-specific NK-92/5.28.z cell line showed reasonable cytotoxic potential against ErbB2-positive tumors, such as glioblastoma[38,39] and RMS[6,10] *in vitro* and *in vivo*. However, singular NK-92/5.28.z cell-mediated immunotherapy may not be sufficient to overcome aRMS resistance. In this study, we explored the effects of the proteasome inhibitor bortezomib[9,40] and combination treatment with bortezomib and CAR-NK-92 cells directed against ErbB2 in preclinical ErbB2-positive aRMS tumor models.

We showed that pretreatment with the proteasome inhibitor bortezomib induced caspase activation in aRMS tumor cell lines RH30 and RH41, but not in the patient-derived aRMS organoid RMS335, and induced cell death in all analyzed RMS cell lines with EC_{50} values in a low nanomolar range between 6.1 and 29.6 nM. We demonstrated a dose-dependent increase in cleaved and activated caspase-3 and -7 in RH30 and RH41 cells. In addition, the expression of the TRAIL-R DR5 on aRMS cells, including the known TRAIL-resistant RH41 cells and the as-yet-unknown TRAIL-resistant RMS335 cells, was upregulated in a dose-dependent manner, whereas DR4 mRNA and protein expression was not induced by bortezomib treatment. Defined aRMS cells, such as the aRMS cell line RH41, are known to be TRAIL resistant,[9] but as has been seen in other cancers, they may be sensitized to TRAIL-mediated cytotoxicity by bortezomib treatment.[30,41]

Combination treatment with bortezomib and NK-92/5.28.z cells resulted in significantly increased lysis of aRMS tumor cells compared to single-agent treatment with NK-92/5.28.z cells.

The NF-κB pathway, a pathway contributing to inflammatory processes with important roles in cancer development and treatment,[42,43] is dependent on proteasomal degradation and therefore might be affected by proteasome inhibition with bortezomib. The proteasome plays important roles in protein turnover, which is essential for

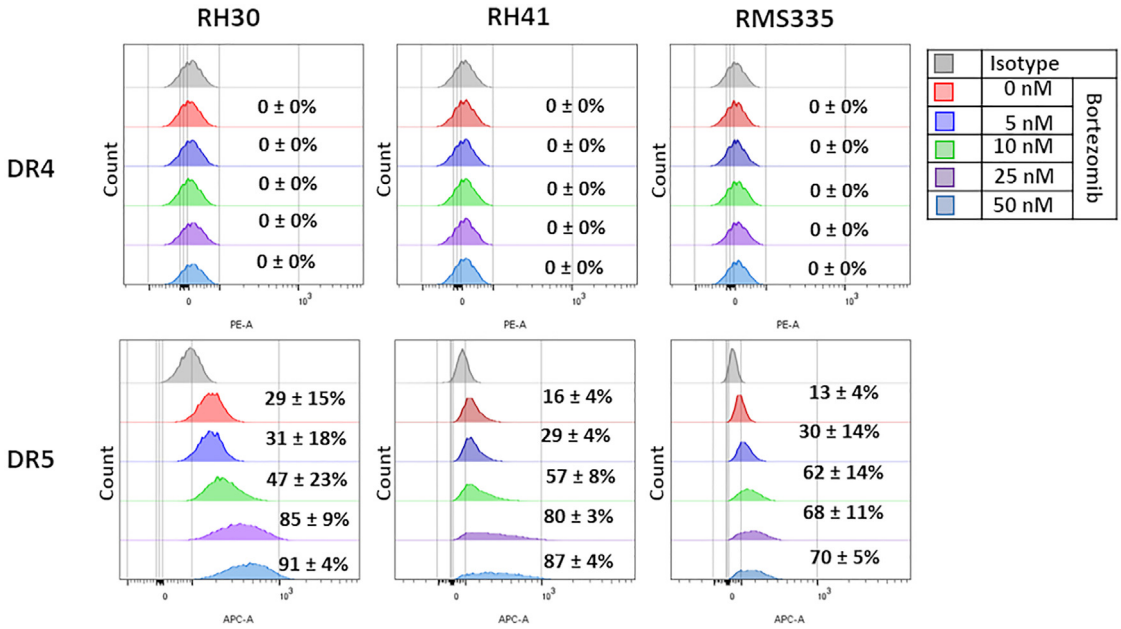

Figure 3. Bortezomib induces the expression of the TRAIL receptor DR5 but not DR4

aRMS cells were incubated for 24 h with the indicated concentrations of bortezomib. The cells were then stained with fluorescence-labeled antibodies against DR4 and DR5. DR4 and DR5 surface expression of the aRMS cell lines RH30, RH41, and RMS335 was analyzed by flow cytometry. Shown is a representative measurement from three independent experiments. A 24 h pretreatment with bortezomib increased the surface expression of DR5, but not DR4, in r/r aRMS cells in a dose-dependent manner.

cellular homeostasis. Bortezomib inhibits the chymotrypsin-like subunit of the 26S proteasome leading to a stabilization of pro-apoptotic factors, causing cellular stress, e.g., endoplasmic reticulum stress and cell-cycle arrest.[44,45] Bortezomib had no influence on p65 mRNA and protein levels, phosphorylation levels, or p100 mRNA and protein expression levels. Treatment with bortezomib, NK-92/5.28.z, or both resulted in an accumulation of p-p100, which might indicate an inhibition of the noncanonical NF-κB pathway. Of note, p52, an NF-κB transcription factor processed from phosphorylated p100 by the 26S proteasome, is considered a driver of cancer progression in different solid tumors.[46–48] Treatment with bortezomib, NK-92/5.28.z cells, or both enhanced the phosphorylation of JNK, a protein kinase involved in pathways that regulate cell proliferation or cell death,[49] indicating increased signaling toward a cell death phenotype in this case. In addition, treatment with NK-92/5.28.z cells and combination treatment with bortezomib both resulted in an increase in caspase-3 activity in aRMS cells. Thus, combination treatment with NK-92/5.28.z cells and the proteasome inhibitor triggers apoptosis by interacting with the NF-κB, JNK, and caspase pathways in aRMS cells.

To exclude intrinsic, non-TRAIL-mediated cytotoxicity of NK-92/5.28.z cells, we performed cytotoxic analyses with a combination treatment of purified TRAIL ligand instead of NK-92/5.28.z cells and bortezomib. We showed synergistic effects in TRAIL-sensitive RH30 cells and initially TRAIL-resistant RMS335 cells. Notably, TRAIL-resistant RH41 cells also responded to the combination treatment and showed at least a tendency toward synergism.

This is the first study of its kind demonstrating increased *in vitro* cytotoxicity of combination treatment with bortezomib and NK-92/5.28.z cells in defined aRMS tumors by enhanced TRAIL-mediated cytotoxicity in, among others, TRAIL-resistant aRMS cells. In our hands, bortezomib demonstrated activity in the concentration range of 5–25 nM, which is below the recommended plasma levels for single-agent therapy in patients with MM, which ranges between 15 and 29 nM (Velcade approval documents).

As it cannot be ruled out that bortezomib treatment may hamper immune cell functions *in vivo*, the timing of bortezomib administration, and therefore the establishment of an *in vivo* model supporting evidence for the findings, might be crucial. In our *in vitro* assays, tumors were cultured in the presence of bortezomib for 24 h before being washed and reseeded in new culture systems without bortezomib. However, the feasibility of combination therapy with bortezomib and CAR-NK-92 treatment has already been demonstrated for renal carcinoma *in vivo*.[24,50]

The clinically usable NK-92/5.28.z cell product has limited *in vivo* persistence due to mandatory irradiation prior to use. Herein, we showed that in terms of r/r aRMS, this limitation can be addressed by combination treatment with the proteasome inhibitor bortezomib. In addition, this combination approach may also increase endogenous T cell responses provided by soluble proinflammatory cytokines *in vivo* in patients, such as IFN-γ, which reverses immunoediting and thereby downregulates HLA class II molecules.[51] Bortezomib treatment may also augment T cell signaling within the TME.[17,52–54]

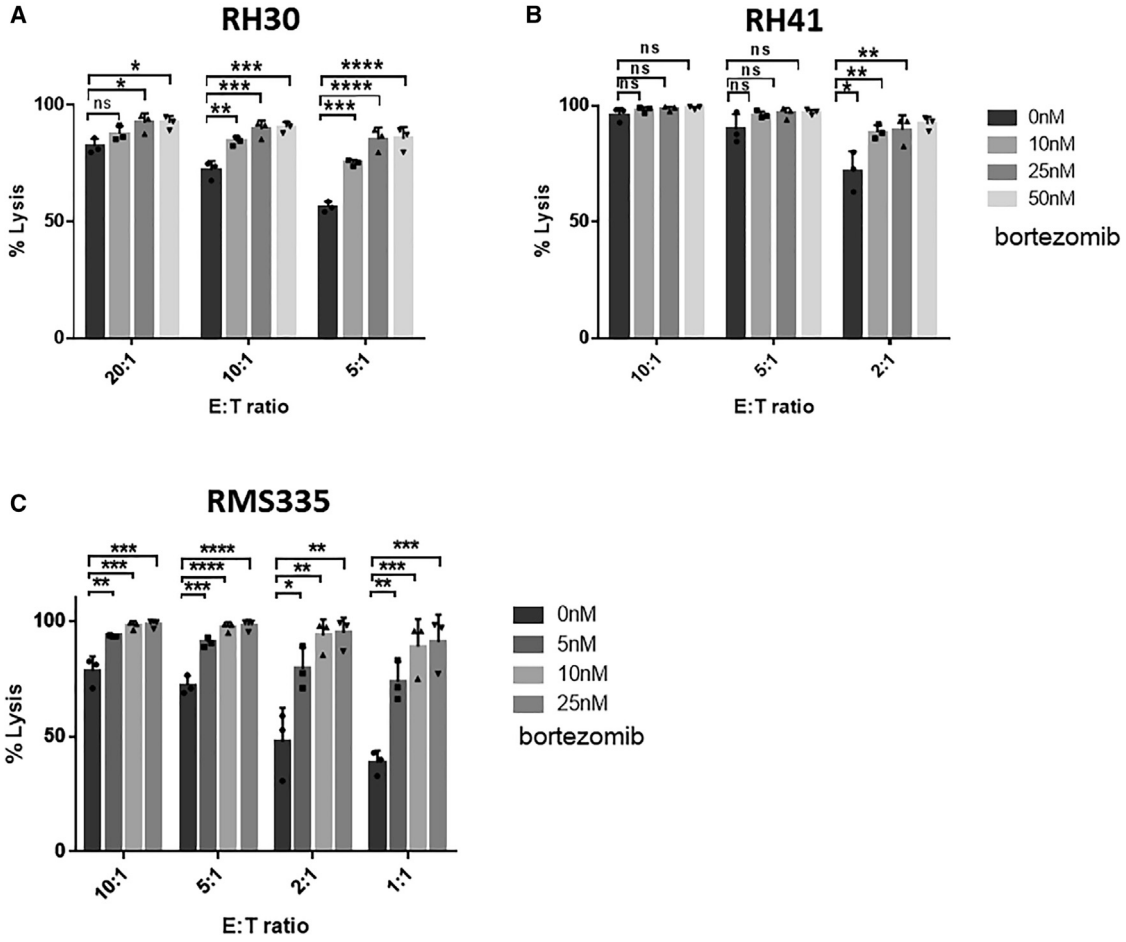

Figure 4. Lysis of bortezomib-pretreated aRMS cells by NK-92/5.28.z cells as assessed by luciferase toxicity assays

aRMS cells RH30 (A), RH41 (B), and RMS335 (C) were treated with the indicated bortezomib concentrations for 24 h. An equal number of cells were then seeded in 96-well plates and co-incubated with NK-92/5.28.z cells for 3 h at different effector-to-target (E:T) cell ratios. Luciferin was added to each well to quantify the luciferase signal of the remaining cells. Based on the signal of the untreated aRMS cells, cell lysis was calculated for each condition. The results of at least three independent experiments are shown. The combination of NK-92/5.28.z immunotherapy with bortezomib significantly increased the lysis of r/r aRMS cells compared to treatment with NK-92/5.28.z cells alone. The results are presented as the mean ± standard deviation (SD), and one-way ANOVA with the Bonferroni method was used to evaluate differences. Differences for $^{*}p < 0.05$, $^{**}p < 0.01$, $^{***}p < 0.005$, and $^{****}p < 0.001$ were considered significant.

Taken together, our studies provide a valid rationale to further explore combination treatment with NK-92/5.28.z cells and bortezomib against r/r aRMS. The combination of bortezomib and NK-92/5.28.z cell therapy, a good manufacturing practice-compliant product that has already been tested in a phase 1 clinical trial for the treatment of relapsed glioblastoma, may be further translated to clinical application to meet the urgent yet unmet medical needs of children and young adults with r/r, metastatic RMS.

MATERIALS AND METHODS

Cell lines

The aRMS cell lines RH30 and RH41 were purchased from DSMZ (Deutsche Sammlung von Mikroorganismen und Zellkuturen GmbH, Braunschweig, Germany). Cells were cultured in RPMI 1640 medium (Gibco, Life Technologies, Carlsbad, CA, USA) supplemented with 10% heat-inactivated fetal bovine serum (Sigma-Aldrich, St. Louis, MO, USA). The patient-derived aRMS tumor organoid RMS335 from a lymph node metastasis of a child with a second relapse of an aRMS tumor was cultured in complete medium BM1* DMEM/F12 (Gibco) containing various growth factors, inhibitors, and additives as reported previously.[55] Then, 0.1%–0.5% basement membrane extract (R&D Systems, Minneapolis, MI, USA) was added to enable cell attachment.

The cytotoxic analyses were performed using a luciferase-based cytotoxicity assay. Luciferase-expressing target cells are used for this assay. Since the viability of the cells correlates directly with the luciferase signal, the luciferase signal can be used to calculate the viability if the signal of the treated cells is related to the signal of the untreated control cells.

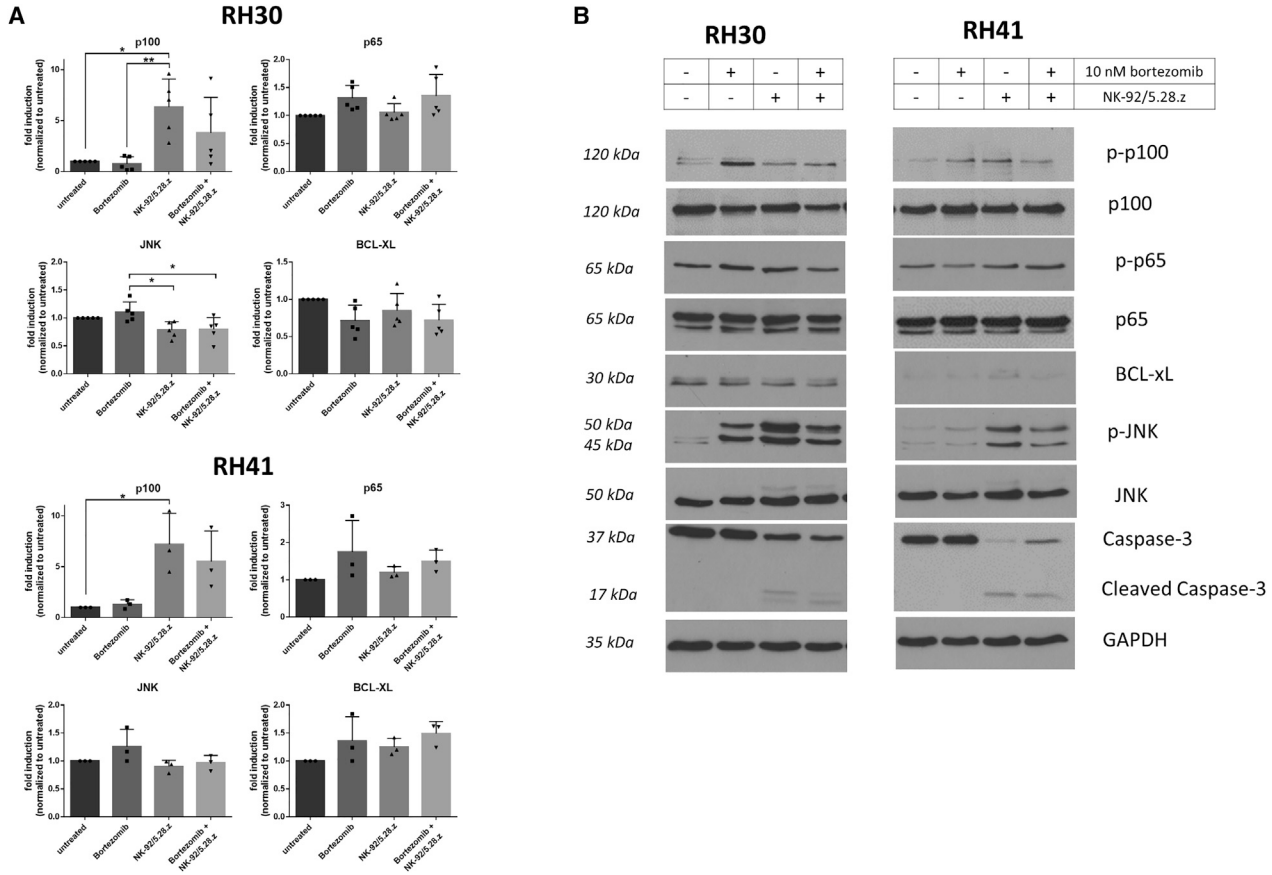

Figure 5. Bortezomib and NK-92/5.28.z cells affect noncanonical NF-κB and JNK signaling in RMS

qPCR analysis of p100, p65, JNK, and BCL-xL mRNA levels in RH30 (A) and RH41 (B) cells upon incubation with or without bortezomib and/or NK-92/5.28.z cells compared to untreated controls. Data are shown of three independent experiments. The results are presented as the mean ± standard deviation (SD), and one-way ANOVA with the Bonferroni method was used to evaluate differences. Differences for $^{*}p < 0.05$, $^{**}p < 0.01$, $^{***}p < 0.005$, and $^{****}p < 0.001$ were considered significant. (C) Western blot analysis of p100, p65, JNK, and the phosphorylated forms of these proteins and BCL-xL, as well as total and cleaved caspase-3, of RH30 and RH41 cells left untreated or treated with bortezomib and/or NK-92/5.28.z cells. GAPDH was used as loading control. Representative blots of two independent experiments are shown.

Stable GFP/firefly luciferase-expressing cell lines were generated by lentiviral transduction with the pSIEW-luc2 plasmid encoding enhanced GFP and firefly luciferase linked by aT2A peptide.[56] If needed, GFP-positive cells were further enriched by fluorescence-activated cell sorting (FACS) with a FACSAria II device (BD Biosciences, San Jose, CA, USA).

The clinically usable NK-92/5.28.z effector cell line was generated by lentiviral transduction of NK-92 cells with an ErbB2-specific CAR construct as described previously.[57,58] The resulting CAR-NK cells express a second-generation CAR containing a single-chain fragment variable domain derived from the ErbB2-specific FRP5 antibody, linked via a modified CD8α hinge region to a CD28-CD3ζ signaling domain. NK-92/5.28.z cells were cultured in X-Vivo10 medium supplemented with recombinant transferrin but without geneticin and phenol red (Lonza, Basel, Switzerland) and 5% human fresh frozen plasma from donors with blood group AB (DRK-Blutspendedienst Frankfurt am Main, Germany) as well as 100 IU/mL interleukin-2 (Proleukin, Novartis, Nuremberg, Germany).

Reagents

Bortezomib was purchased from AbMole BioScience and was dissolved in DMSO at a stock concentration of 10 mM and further diluted to 1 mM in Dulbecco's phosphate-buffered saline (DPBS) (Gibco). Stock solutions were stored at −20°C. For each experiment, fresh 1 mM stocks were thawed, diluted in medium, and used immediately.

EC_{50} value determination

For EC_{50} determination, the luciferase-based viability assay was used as previously described.[10] A total of 5,000 luciferase-expressing RMS cells were seeded in white 96-well plates, and bortezomib was added at concentrations ranging from 0 to 1 mM. Cells were

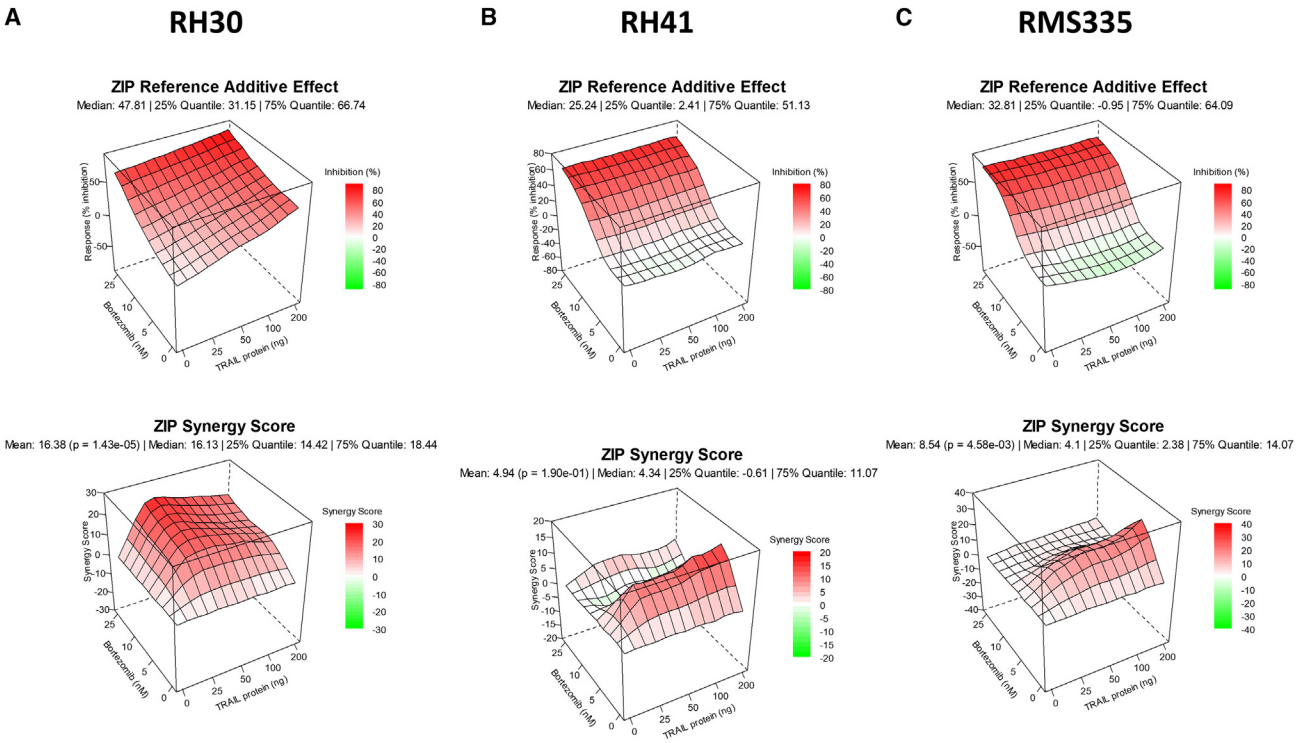

Figure 6. Synergistic interactions between bortezomib and TRAIL treatment

Luciferase-based cytotoxicity assays were performed with bortezomib-pretreated aRMS cells and purified TRAIL protein. The results were used in a zero interaction potency (ZIP) model to analyze additive or synergistic effects. For RH30 cells (A), RH41 cells (B), and RMS335 cells (C), the ZIP reference for additive effects (top row) was modeled, showing the expected effects when bortezomib and TRAIL have an additive effect. In addition, the synergy score (bottom row) was used, indicating the actual interactions between the two drugs. Overall, the ZIP additive model calculated the expected response of a combination treatment with bortezomib and TRIAL based on the potency of the individual therapies and the sum of the individual effects (additive) without any interaction. The ZIP synergy score was calculated by comparing the observed combined effect of bortezomib and TRIAL with the expected individual effects (from the ZIP reference model). The observed combined effect of bortezomib and TRIAL was increased compared to the sum of the monotherapies, resulting in a positive score indicating a synergetic interaction between bortezomib and TRIAL.

incubated for 24 or 48 h before D-luciferin (Promega, Madison, WI, USA) was added at a final concentration of 0.5 mM. After 15 min incubation, light emission was quantified by a GloMax-Multi Detection device (Promega), and tumor cell lysis was calculated by quantifying the intracellular luciferase activity of living cells using the following formula:

$$\%\ Specific\ lysis\ = \left(1 - \frac{Remaining\ target\ cells\ (signal)}{Negative\ control\ (signal)}\right) x\ 100\%$$

The results of at least three experiments were used for dose-response curves and the calculated EC_{50} to measure drug effects.

Levels of DR4 and DR5 surface expression on aRMS cells

The aRMS target cells were cultured in the presence of 0–100 nM bortezomib. After 24 h incubation, target cells were harvested and placed in FACS tubes. After washing with DPBS according to the manufacturer's instructions, the cells were stained with antibodies against TRAIL-Rs DR4 and DR5 conjugated to phycoerythrin (BioLegend, San Diego, CA, USA), allophycocyanin (BioLegend), or isotype controls (BioLegend). Target cells were analyzed by a FACS Canto10c (BD Biosciences), and data were evaluated by FlowJo software (v.10.8.1, TreeStar, Ashland, OR, USA).

Caspase activity assay

Caspase activity of bortezomib-treated aRMS cells was analyzed by Caspase-Glo assay (Promega). A total of 500,000 aRMS cells were seeded per well on a 6-well plate and incubated with 5, 10, or 25 nM bortezomib for 24 h. As a positive control, cells were treated with 1 μM staurosporine, and as a negative control, untreated cells were used. All cells were seeded at a density of 10,000 cells per well on a white 96-well plate, and Caspase-Glo 3/7 reagent was added. After 1 h, luminescence was recorded with a GloMax-Multi Detection device (Promega) according to the manufacturer's instructions.

Western blotting

aRMS RH30 and RH41 cells were treated with 0, 5, 10, or 25 nM bortezomib for 24 h. Cells were lysed in radioimmunoprecipitation assay (RIPA) lysis buffer (50 mM Tris-HCl [pH 8], 150 mM NaCl, 1% Nonidet P-40, 2 mM MgCl2, 0.5% sodium deoxycholate)

supplemented with protease inhibitor complex (Roche, Grenzach, Germany), 0.1% SDS, 1 mM sodium orthovanadate, 5 mM sodium fluoride, 1 mM β-glycerophosphate, 1 mM phenylmethylsulfonyl fluoride, and Pierce Universal Nuclease (Thermo Fisher Scientific) for 30 min on ice. The lysates were cleared by centrifugation for 20 min at 18,000 × *g* and 4°C. Protein concentrations were determined using the bicinchoninic acid (BCA) Protein Assay Kit from Pierce (Thermo Scientific) according to the manufacturer's protocol, and 30–40 μg protein was boiled in 6× SDS loading buffer (350 mM Tris base [pH 6.8], 38% glycerol, 10% SDS, 93 mg/mL dithiothreitol, 120 mg/mL bromophenol blue) followed by western blotting. Membranes were blocked with 5% milk powder in PBS-T for 1 h and incubated with antibodies overnight at 4°C. The following primary antibodies were used in this study: rabbit anti-phospho NF-κB2 p100 (Ser866/870) (4810, Cell Signaling Technology); mouse anti-NF-κB p52 (05-361, Merck/Sigma); rabbit anti-phospho JNK1/2 (Thr183/Tyr185) (44-682G, Thermo Scientific); rabbit anti-JNK1 (44-690G, Thermo Scientific); rabbit anti-phospho-NF-κB p65 (Ser536) (3033, Cell Signaling Technology); mouse anti-NF-κB p65 (sc-8008, Santa Cruz Biotechnology); rabbit anti-caspase-3 (9662, Cell Signaling Technology); rabbit anti-Bcl-XL (2762, Cell Signaling Technology); mouse anti-GAPDH (5G4 cc, HyTest, Turku, Finland); and mouse anti-Vinculin (V9131, Merck KGaA). The following horseradish peroxidase (HRP)-coupled secondary antibodies were used for detection with Pierce ECL western blotting substrate (Thermo Scientific): HRP-conjugated goat anti-mouse IgG (ab6789, Abcam) and HRP-conjugated goat anti-rabbit IgG (ab6721, Abcam). Representative blots of at least two independent experiments are shown. Only one loading control is shown for clarity if samples from one experiment were detected on multiple western blotting membranes.

Furthermore, RH30 and RH41 cell lysates after combination treatment with bortezomib and NK-92/5.28.z were analyzed by western blotting. For this, aRMS cells were pretreated with 10 nM bortezomib for 24 h and subsequently coincubated with NK-92/5.28.z cells at an effector-to-target (E:T) ratio of 1:1 for 2 h. aRMS cells treated with either the single agent bortezomib or NK-92/5.28.z, and untreated controls were used as references. Western blotting was performed as described above.

qPCR

For qPCR analysis, aRMS cells were seeded in 6-well plates and pretreated with 10 nM bortezomib for 24 h. Pre- or untreated target cells were seeded at densities of 5×10^5 cells per well on 6-well plates, and NK-92/5.28.z effector cells were added at E:T ratios of 1:1. Altogether, untreated, 10 nM bortezomib-treated, NK-92/5.28.z cell-treated, and 10 nM bortezomib plus NK-92/5.28.z cell-treated target cells were cultured for 2 h, washed with DPBS, and stored at −80°C until further use.

RNA isolation was performed using the peqGOLD total RNA isolation kit (VWR, Radnor, PA, USA) according to the manufacturer's protocol. Cell lysates were prepared using RNA lysis buffer and then transferred to peqGOLD RNA homogenizer columns. After centrifugation at 13,000 × *g* for 1 min, the filtrate was mixed with 70% ethanol, loaded onto a peqGOLD RNA mini column, and centrifuged at 10,000 × *g* for 1 min, followed by a wash step with RNA wash buffer and two wash steps with 80% ethanol (centrifugation at 10,000 × *g*). The columns were dried by centrifugation at 12,000 × *g* for 2 min, and RNA was eluted in nuclease-free water (centrifugation at 12,000 × *g* for 2 min). RNA (0.5 μg) was used for cDNA synthesis using the RevertAid H Minus First Strand Kit (Thermo Scientific) according to the manufacturer's protocol. The gene expression levels of DR4, DR5, p100, p65, JNK, and BCL-XL were determined by SYBR green-based real-time qPCR using the 7900GR Fast Real-time PCR system (Applied Biosystems, Darmstadt, Germany). Gene expression data for target genes were normalized against 18S-rRNA or RPII expression, and relative gene expression levels were calculated using the $2^{-\Delta\Delta Ct}$ method. All primers used in this study were obtained from Eurofins (Hamburg, Germany) and are listed here: DR4: forward 5′-TGTTGCATCGGCTC AGGTTG-3′, reverse 5′-ACGAAAGTGGACAGCGAGTC-3′; DR5: forward 5′-CAGGTGTGATTCAGGTGAAGTG-3′, reverse 5′-CCCA CTGTGCTTTGTACCTG-3′; p100: forward 5′-GAGGGCCTTTAGC GGACAG-3′, reverse 5′-CGGGTCCGCGTATCTTTGTA-3′; p65: forward 5′-GCCGAGTGAACCGAAACTCT-3′, reverse 5′-GCCTGG TCCCGTGAAATACA-3′; JNK: forward 5′-CTGAAGCAGAAGC TCCACCA-3′, reverse 5′-TGCACCTAAAGGAGAGGGCT-3′; BCL-XL: forward 5′-CTGAATCGGAGATGGAGACC-3′, reverse 5′-TGGG ATGTCAGGTCACTGAA-3′; 18S: forward 5′-CGCAAATTACCCA CTCCCG-3′, reverse 5′-TTCCAATTACAGGGCCTCGAA-3′; and RPII: forward 5′-GCACCACGTCCAATGACAT-3′, reverse 5′-GTGC GGCTGCTTCCATAA-3′.

Combination of bortezomib and immunotherapy

Luciferase-expressing aRMS cells were pretreated with 0, 5, 10, or 25 nM bortezomib for 24 h before seeding them on white 96-well plates at densities of 7,500 cells per well. After adherence of target cells, NK-92/5.28.z effector cells were added at E:T ratios of 20:1, 10:1, 5:1, 2:1, and 1:1. After a 3 h coculture period, luciferase signals of the remaining cells were determined by adding 0.5 mM D-luciferin (Promega) for 15 min. Luciferase signals were quantified with a GloMax-Multi Detection device (Promega), and specific target cell lysis was calculated according to the formula mentioned above.

TRAIL cytotoxicity assay

A total of 5,000 luciferase-expressing aRMS cells were seeded per well on white 96-well plates. After cell adherence, 0, 5, 10, or 25 nM bortezomib and 0, 25, 50, 100, or 200 ng/mL purified TRAIL protein (BioLegend) were added. After 20 h, 0.5 mM D-luciferin solution was added and incubated for another 15 min. The luminescence signal was detected by a GloMax-Multi Detection device (Promega), and specific lysis of target cells was calculated according to the formula mentioned above.

Statistical analysis

For statistical analysis and graphical presentation of data, GraphPad PRISM 6.0 software (La Jolla, CA, USA) was used. The results are

presented as the mean ± standard deviation (SD), and one-way ANOVA with the Bonferroni method was used to evaluate differences. Differences for $^{*}p < 0.05$, $^{**}p < 0.01$, $^{***}p < 0.005$, and $^{****}p < 0.001$ were considered significant. Flow cytometry data are given as the percentage of gated cells as the mean ± SD in the case of replicated data. The degree of synergy of simultaneous bortezomib and TRAIL treatment was calculated by the ZIP model.[59] This model was chosen because it combines the advantages of the Loewe additivity and Bliss independence models. The ZIP model is a reference model for calculating the expected effect of a drug combination. It assumes that the individual drugs do not influence the efficacy of each other. The expected effect of a drug combination is calculated as the sum of the effects of the individual drugs (additive, includes the effect when there is no interaction between the drugs). The degree of synergy or antagonism of the drug combination is quantified by comparing the observed response of the drug combination with the expected response calculated using the ZIP model. The ZIP synergy score is a measure of the degree of synergy or antagonism between two drugs. It is calculated by comparing the observed response of the drug combination with the expected response calculated using the ZIP model. If the observed response is greater than the expected response, then the ZIP synergy score is positive, indicating synergy. If the observed response is less than the expected response, then the ZIP synergy score is negative, indicating antagonism. If the observed response is equal to the expected response, then the ZIP synergy score is zero, indicating additivity.[59]

DATA AND CODE AVAILABILITY

The original contributions presented in the study are included in the article/supplemental information, and further inquiries can be directed to the corresponding author.

ACKNOWLEDGMENTS

We would like to explicitly thank Michael T. Meister and Jano Drost for providing the patient-derived tumor organoid cell line RMS335 and for their support. This research was funded by the LOEWE-FCI, Frankfurt Cancer Institute, Frankfurt am Main, Germany, funded by the Hessian Ministry of Higher Education, Research and the Arts (2019). This work was also supported by grants from the Else Kröner Fresenius-Stiftung (to L.M.M.), the Mildred-Scheel-Nachwuchszentrum (MSNZ), Frankfurt am Main, Germany (to E.R., 70113301), and the Schwiete Stiftung (Projekt Nr. 2021-012) and by grants from the Parents Association "Hilfe für krebskranke-Kinder e.V.," Frankfurt am Main, Germany. J.-H.K. receives funding from the European Research Council (ERC) under the European Union's Horizon 2020 Research and Innovation Programme (grant agreement no. 714226). Research in the laboratory of S.J.L.v.W. is supported by the Deutsche Forschungsgemeinschaft (DFG) (WI 5171/1-1, WI 5171/4-1, FU 436/20-1, FU 436/21-1, and project-ID 259130777 – CRC1177), the Deutsche Krebshilfe (70113680), Wilhelm Sander-Stiftung (2020.008.1), the Frankfurter Stiftung für krebskranke Kinder, and the Dr. Eberhard and Hilde Rüdiger Foundation. This work was also supported by Association "Help for Children with Cancer e.V." as part of the C^{3}OMBAT consortium (E.S.-M., E.R., and J.-H.K.).

AUTHOR CONTRIBUTIONS

C.H., L.H., N.W., L.M.M., S.J.L.v.W., M.M., and E.R. conceived and designed the experiments. C.H., L.H., N.W., L.M.M., and E.R. performed the experiments. C.H., L.H., N.W., L.M.M., E.S.-M., S.J.L.v.W., M.M., and E.R. analyzed the data. T.T., W.S.W., S.J.L.v.W., E.R., J.-H.K., and P.B. contributed reagents, materials, and analysis tools. C.H. and E.R. wrote the manuscript. L.H., N.W., L.M.M., T.T., W.S.W., J.-H.K., S.J.L.v.W., P.B., and M.M. revised the manuscript. J.-H.K. and P.B. supervised the research. The final draft of the manuscript was approved by all coauthors.

DECLARATION OF INTERESTS

J.-H.K. has advisory roles for Bluebird Bio, Novartis, Roche, and Jazz Pharmaceuticals. T.T. and W.S.W. are named as inventors on patents and patent applications related to the therapeutic agent used in this study, owned by their respective academic institutions.

REFERENCES

1. Perez, E.A., Kassira, N., Cheung, M.C., Koniaris, L.G., Neville, H.L., and Sola, J.E. (2011). Rhabdomyosarcoma in children: a SEER population based study. J. Surg. Res. *170*, e243–e251. https://doi.org/10.1016/j.jss.2011.03.001.

2. Gurria, J.P., and Dasgupta, R. (2018). Rhabdomyosarcoma and Extraosseous Ewing Sarcoma. Children *5*, 165. https://doi.org/10.3390/children5120165.

3. Dasgupta, R., Fuchs, J., and Rodeberg, D. (2016). Rhabdomyosarcoma. Semin. Pediatr. Surg. *25*, 276–283. https://doi.org/10.1053/j.sempedsurg.2016.09.011.

4. Pan, K., Farrukh, H., Chittepu, V.C.S.R., Xu, H., Pan, C.-X., and Zhu, Z. (2022). CAR race to cancer immunotherapy: from CAR T, CAR NK to CAR macrophage therapy. J. Exp. Clin. Cancer Res. *41*, 119. https://doi.org/10.1186/s13046-022-02327-z.

5. Varlet, P., Bouffet, E., Casanova, M., Giangaspero, F., Antonelli, M., Hargrave, D., Ladenstein, R., Pearson, A., Hawkins, C., König, F.B., et al. (2022). Comprehensive analysis of the ErbB receptor family in pediatric nervous system tumors and rhabdomyosarcoma, Pediatr. Blood Cancer *69*, e29316. https://doi.org/10.1002/pbc.29316.

6. Gossel, L.D.H., Heim, C., Pfeffermann, L.-M., Moser, L.M., Bönig, H.B., Klingebiel, T.E., Bader, P., Wels, W.S., Merker, M., and Rettinger, E. (2021). Retargeting of NK-92 Cells against High-Risk Rhabdomyosarcomas by Means of an ERBB2 (HER2/Neu)-Specific Chimeric Antigen Receptor. Cancers *13*, 1443. https://doi.org/10.3390/cancers13061443.

7. Prager, I., and Watzl, C. (2019). Mechanisms of natural killer cell-mediated cellular cytotoxicity. J. Leukoc. Biol. *105*, 1319–1329. https://doi.org/10.1002/JLB.MR0718-269R.

8. Benmebarek, M.-R., Karches, C.H., Cadilha, B.L., Lesch, S., Endres, S., and Kobold, S. (2019). Killing Mechanisms of Chimeric Antigen Receptor (CAR) T Cells. Int. J. Mol. Sci. *20*, 1283. https://doi.org/10.3390/ijms20061283.

9. Petak, I., Douglas, L., Tillman, D.M., Vernes, R., and Houghton, J.A. (2000). Pediatric rhabdomyosarcoma cell lines are resistant to Fas-induced apoptosis and highly sensitive to TRAIL-induced apoptosis. Clin. Cancer Res. *6*, 4119–4127.

10. Heim, C., Moser, L.M., Kreyenberg, H., Bönig, H., Tonn, T., Wels, W.S., Gradhand, E., Ullrich, E., Meister, M.T., Koerkamp, M.G., et al. (2023). ErbB2 (HER2)-CAR-NK-92 cells for enhanced immunotherapy of metastatic fusion-driven alveolar rhabdomyosarcoma. Front. Immunol. *14*, 1228894. https://doi.org/10.3389/fimmu.2023.1228894.

11. Adams, J. (2001). Proteasome inhibition in cancer: Development of PS-341. Semin. Oncol. *28*, 613–619. https://doi.org/10.1016/S0093-7754(01)90034-X.

12. Teicher, B.A., Ara, G., Herbst, R., Palombella, V.J., and Adams, J. (1999). The proteasome inhibitor PS-341 in cancer therapy. Clin. Cancer Res. *5*, 2638–2645.

13. Boccadoro, M., Morgan, G., and Cavenagh, J. (2005). Preclinical evaluation of the proteasome inhibitor bortezomib in cancer therapy. Cancer Cell Int. *5*, 18. https://doi.org/10.1186/1475-2867-5-18.

14. Milano, A., Iaffaioli, R.V., and Caponigro, F. (2007). The proteasome: a worthwhile target for the treatment of solid tumours? Eur. J. Cancer *43*, 1125–1133. https://doi.org/10.1016/j.ejca.2007.01.038.

15. Baou, M., Kohlhaas, S.L., Butterworth, M., Vogler, M., Dinsdale, D., Walewska, R., Majid, A., Eldering, E., Dyer, M.J.S., and Cohen, G.M. (2010). Role of NOXA and its ubiquitination in proteasome inhibitor-induced apoptosis in chronic lymphocytic leukemia cells. Haematologica *95*, 1510–1518. https://doi.org/10.3324/haematol.2010.022368.

16. Maki, R.G., Kraft, A.S., Scheu, K., Yamada, J., Wadler, S., Antonescu, C.R., Wright, J.J., and Schwartz, G.K. (2005). A multicenter Phase II study of bortezomib in recurrent or metastatic sarcomas. Cancer *103*, 1431–1438. https://doi.org/10.1002/cncr.20968.

17. Ames, E., Hallett, W.H.D., and Murphy, W.J. (2009). Sensitization of human breast cancer cells to natural killer cell-mediated cytotoxicity by proteasome inhibition. Clin. Exp. Immunol. *155*, 504–513. https://doi.org/10.1111/j.1365-2249.2008.03818.x.

18. Hellwig, C.T., Delgado, M.E., Skoko, J., Dyck, L., Hanna, C., Wentges, A., Langlais, C., Hagenlocher, C., Mack, A., Dinsdale, D., et al. (2022). Proteasome inhibition triggers the formation of TRAIL receptor 2 platforms for caspase-8 activation that accumulate in the cytosol. Cell Death Differ. *29*, 147–155. https://doi.org/10.1038/s41418-021-00843-7.

19. Takeda, K., Smyth, M.J., Cretney, E., Hayakawa, Y., Kayagaki, N., Yagita, H., and Okumura, K. (2002). Critical role for tumor necrosis factor-related apoptosis-inducing ligand in immune surveillance against tumor development. J. Exp. Med. *195*, 161–169. https://doi.org/10.1084/jem.20011171.

20. Srivastava, R.K. (2001). TRAIL/Apo-2L: mechanisms and clinical applications in cancer. Neoplasia *3*, 535–546. https://doi.org/10.1038/sj.neo.7900203.

21. Zhang, L., and Fang, B. (2005). Mechanisms of resistance to TRAIL-induced apoptosis in cancer. Cancer Gene Ther. *12*, 228–237. https://doi.org/10.1038/sj.cgt.7700792.

22. Koschny, R., Ganten, T.M., Sykora, J., Haas, T.L., Sprick, M.R., Kolb, A., Stremmel, W., and Walczak, H. (2007). TRAIL/bortezomib cotreatment is potentially hepatotoxic but induces cancer-specific apoptosis within a therapeutic window. Hepatology *45*, 649–658. https://doi.org/10.1002/hep.21555.

23. Gras Navarro, A., Espedal, H., Joseph, J.V., Trachsel-Moncho, L., Bahador, M., Gjertsen, B.T., Kristoffersen, E.K., Simonsen, A., Miletic, H., Enger, P.Ø., et al. (2019). Pretreatment of Glioblastoma with Bortezomib Potentiates Natural Killer Cell Cytotoxicity through TRAIL/DR5 Mediated Apoptosis and Prolongs Animal Survival. Cancers *11*, 996. https://doi.org/10.3390/cancers11070996.

24. Zhang, Q., Xu, J., Ding, J., Liu, H., Li, H., Li, H., Lu, M., Miao, Y., Wang, Z., Fu, Q., and Zheng, J. (2018). Bortezomib improves adoptive carbonic anhydrase IX-specific chimeric antigen receptor-modified NK92 cell therapy in mouse models of human renal cell carcinoma. Oncol. Rep. *40*, 3714–3724. https://doi.org/10.3892/or.2018.6731.

25. Meister, M.T., Groot Koerkamp, M.J.A., de Souza, T., Breunis, W.B., Frazer-Mendelewska, E., Brok, M., DeMartino, J., Manders, F., Calandrini, C., Kerstens, H.H.D., et al. (2022). Mesenchymal tumor organoid models recapitulate rhabdomyosarcoma subtypes. EMBO Mol. Med. *14*, e16001. https://doi.org/10.15252/emmm.202216001.

26. Hinson, A.R.P., Jones, R., Crose, L.E.S., Belyea, B.C., Barr, F.G., and Linardic, C.M. (2013). Human rhabdomyosarcoma cell lines for rhabdomyosarcoma research: utility and pitfalls. Front. Oncol. *3*, 183. https://doi.org/10.3389/fonc.2013.00183.

27. Wakuri, S., Yamakage, K., Kazuki, Y., Kazuki, K., Oshimura, M., Aburatani, S., Yasunaga, M., and Nakajima, Y. (2017). Correlation between luminescence intensity and cytotoxicity in cell-based cytotoxicity assay using luciferase. Anal. Biochem. *522*, 18–29. https://doi.org/10.1016/j.ab.2017.01.015.

28. Qureshi, M.Z., Romero, M.A., Attar, R., Javed, Z., and Farooqi, A.A. (2015). TRAIL and Bortezomib: killing cancer with two stones. Asian Pac. J. Cancer Prev. *16*, 1671–1674. https://doi.org/10.7314/apjcp.2015.16.4.1671.

29. de Wilt, L.H.A.M., Kroon, J., Jansen, G., de Jong, S., Peters, G.J., and Kruyt, F.A.E. (2013). Bortezomib and TRAIL: a perfect match for apoptotic elimination of tumour cells? Crit. Rev. Oncol. Hematol. *85*, 363–372. https://doi.org/10.1016/j.critrevonc.2012.08.001.

30. Koschny, R., Holland, H., Sykora, J., Erdal, H., Krupp, W., Bauer, M., Bockmuehl, U., Ahnert, P., Meixensberger, J., Stremmel, W., et al. (2010). Bortezomib sensitizes primary human esthesioneuroblastoma cells to TRAIL-induced apoptosis. J. Neurooncol. *97*, 171–185. https://doi.org/10.1007/s11060-009-0010-6.

31. Li, Q., and Verma, I.M. (2002). NF-kappaB regulation in the immune system. Nat. Rev. Immunol. *2*, 725–734. https://doi.org/10.1038/nri910.

32. Heske, C.M., and Mascarenhas, L. (2021). Relapsed Rhabdomyosarcoma. J. Clin. Med. *10*, 804. https://doi.org/10.3390/jcm10040804.

33. Hegde, M., Joseph, S.K., Pashankar, F., DeRenzo, C., Sanber, K., Navai, S., Byrd, T.T., Hicks, J., Xu, M.L., Gerken, C., et al. (2020). Tumor response and endogenous immune reactivity after administration of HER2 CAR T cells in a child with metastatic rhabdomyosarcoma. Nat. Commun. *11*, 3549. https://doi.org/10.1038/s41467-020-17175-8.

34. Ganti, R., Skapek, S.X., Zhang, J., Fuller, C.E., Wu, J., Billups, C.A., Breitfeld, P.P., Dalton, J.D., Meyer, W.H., and Khoury, J.D. (2006). Expression and genomic status of EGFR and ErbB-2 in alveolar and embryonal rhabdomyosarcoma. Mod. Pathol. *19*, 1213–1220. https://doi.org/10.1038/modpathol.3800636.

35. D'Agostino, S., Tombolan, L., Saggioro, M., Frasson, C., Rampazzo, E., Pellegrini, S., Favaretto, F., Biz, C., Ruggieri, P., Gamba, P., et al. (2020). Rhabdomyosarcoma Cells Produce Their Own Extracellular Matrix With Minimal Involvement of Cancer-Associated Fibroblasts: A Preliminary Study. Front. Oncol. *10*, 600980. https://doi.org/10.3389/fonc.2020.600980.

36. Kather, J.N., Hörner, C., Weis, C.-A., Aung, T., Vokuhl, C., Weiss, C., Scheer, M., Marx, A., and Simon-Keller, K. (2019). CD163+ immune cell infiltrates and presence of CD54+ microvessels are prognostic markers for patients with embryonal rhabdomyosarcoma. Sci. Rep. *9*, 9211. https://doi.org/10.1038/s41598-019-45551-y.

37. DeMartino, J., Meister, M.T., Visser, L., Brok, M., Groot Koerkamp, M.J.A., Hiemcke-Jiwa, L.S., De Souza, T., Merks, J.H.M., Holstege, F.C.P., Margaritis, T., et al. (2022). Single-cell Transcriptomics Reveals Immune Suppression and Cell States Predictive of Patient Outcomes in Rhabdomyosarcoma.

38. Zhang, C., Burger, M.C., Jennewein, L., Genßler, S., Schönfeld, K., Zeiner, P., Hattingen, E., Harter, P.N., Mittelbronn, M., Tonn, T., et al. (2016). ErbB2/HER2-Specific NK Cells for Targeted Therapy of Glioblastoma. J. Natl. Cancer Inst. *108*. https://doi.org/10.1093/jnci/djv375.

39. Burger, M.C., Zhang, C., Harter, P.N., Romanski, A., Strassheimer, F., Senft, C., Tonn, T., Steinbach, J.P., and Wels, W.S. (2019). CAR-Engineered NK Cells for the Treatment of Glioblastoma: Turning Innate Effectors Into Precision Tools for Cancer Immunotherapy. Front. Immunol. *10*, 2683. https://doi.org/10.3389/fimmu.2019.02683.

40. Bersani, F., Taulli, R., Accornero, P., Morotti, A., Miretti, S., Crepaldi, T., and Ponzetto, C. (2008). Bortezomib-mediated proteasome inhibition as a potential strategy for the treatment of rhabdomyosarcoma. Eur. J. Cancer *44*, 876–884. https://doi.org/10.1016/j.ejca.2008.02.022.

41. Jane, E.P., Premkumar, D.R., and Pollack, I.F. (2011). Bortezomib sensitizes malignant human glioma cells to TRAIL, mediated by inhibition of the NF-{kappa}B signaling pathway. Mol. Cancer Ther. *10*, 198–208. https://doi.org/10.1158/1535-7163.MCT-10-0725.

42. Xia, L., Tan, S., Zhou, Y., Lin, J., Wang, H., Oyang, L., Tian, Y., Liu, L., Su, M., Wang, H., et al. (2018). Role of the NFκB-signaling pathway in cancer. Onco. Targets Ther. *11*, 2063–2073. https://doi.org/10.2147/OTT.S161109.

43. Liu, T., Zhang, L., Joo, D., and Sun, S.-C. (2017). NF-κB signaling in inflammation. Signal Transduct. Target. Ther. *2*, 17023. https://doi.org/10.1038/sigtrans.2017.23.

44. Chen, D., Frezza, M., Schmitt, S., Kanwar, J., and Dou, Q.P. (2011). Bortezomib as the first proteasome inhibitor anticancer drug: current status and future perspectives. Curr. Cancer Drug Targets *11*, 239–253. https://doi.org/10.2174/156800911794519752.

45. Ito, S. (2020). Proteasome Inhibitors for the Treatment of Multiple Myeloma. Cancers *12*, 265. https://doi.org/10.3390/cancers12020265.

46. Wright, K.D., Miller, B.S., El-Meanawy, S., Tsaih, S.-W., Banerjee, A., Geurts, A.M., Sheinin, Y., Sun, Y., Kalyanaraman, B., Rui, H., et al. (2019). The p52 isoform of SHC1

is a key driver of breast cancer initiation. Breast Cancer Res. *21*, 74. https://doi.org/10.1186/s13058-019-1155-7.

47. Saxon, J.A., Yu, H., Polosukhin, V.V., Stathopoulos, G.T., Gleaves, L.A., McLoed, A.G., Massion, P.P., Yull, F.E., Zhao, Z., and Blackwell, T.S. (2018). p52 expression enhances lung cancer progression. Sci. Rep. *8*, 6078. https://doi.org/10.1038/s41598-018-24488-8.

48. Hufnagel, D.H., Wilson, A.J., Saxon, J., Blackwell, T.S., Watkins, J., Khabele, D., Crispens, M.A., Yull, F.E., and Beeghly-Fadiel, A. (2020). Expression of p52, a non-canonical NF-kappaB transcription factor, is associated with poor ovarian cancer prognosis. Biomark. Res. *8*, 45. https://doi.org/10.1186/s40364-020-00227-y.

49. Tournier, C. (2013). The 2 Faces of JNK Signaling in Cancer. Genes Cancer *4*, 397–400. https://doi.org/10.1177/1947601913486349.

50. Kang, Z., Chen, J.-J., Yu, Y., Li, B., Sun, S.-Y., Zhang, B., and Cao, L. (2011). Drozitumab, a human antibody to death receptor 5, has potent antitumor activity against rhabdomyosarcoma with the expression of caspase-8 predictive of response. Clin. Cancer Res. *17*, 3181–3192. https://doi.org/10.1158/1078-0432.CCR-10-2874.

51. Castro, F., Cardoso, A.P., Gonçalves, R.M., Serre, K., and Oliveira, M.J. (2018). Interferon-Gamma at the Crossroads of Tumor Immune Surveillance or Evasion. Front. Immunol. *9*, 847. https://doi.org/10.3389/fimmu.2018.00847.

52. Thounaojam, M.C., Dudimah, D.F., Pellom, S.T., Uzhachenko, R.V., Carbone, D.P., Dikov, M.M., and Shanker, A. (2015). Bortezomib enhances expression of effector molecules in anti-tumor CD8+ T lymphocytes by promoting Notch-nuclear factor-κB crosstalk. Oncotarget *6*, 32439–32455. https://doi.org/10.18632/oncotarget.5857.

53. Pellom, S.T., Dudimah, D.F., Thounaojam, M.C., Uzhachenko, R.V., Singhal, A., Richmond, A., and Shanker, A. (2017). Bortezomib augments lymphocyte stimulatory cytokine signaling in the tumor microenvironment to sustain CD8+T cell antitumor function. Oncotarget *8*, 8604–8621. https://doi.org/10.18632/oncotarget.14365.

54. Mohty, M., Brissot, E., Savani, B.N., and Gaugler, B. (2013). Effects of bortezomib on the immune system: a focus on immune regulation. Biol. Blood Marrow Transpl. *19*, 1416–1420. https://doi.org/10.1016/j.bbmt.2013.05.011.

55. Meister, M.T., Groot Koerkamp, M.J., de Souza, T., Breunis, W.B., Frazer-Mendelewska, E., Brok, M., DeMartino, J., Manders, F., Calandrini, C., Kerstens, H.H., et al. (2022). Mesenchymal Tumor Organoid Models Recapitulate Rhabdomyosarcoma Subtypes (Cold Spring Harbor Laboratory).

56. Abel, T., El Filali, E., Waern, J., Schneider, I.C., Yuan, Q., Münch, R.C., Hick, M., Warnecke, G., Madrahimov, N., Kontermann, R.E., et al. (2013). Specific gene delivery to liver sinusoidal and artery endothelial cells. Blood *122*, 2030–2038. https://doi.org/10.1182/blood-2012-11-468579.

57. Schönfeld, K., Sahm, C., Zhang, C., Naundorf, S., Brendel, C., Odendahl, M., Nowakowska, P., Bönig, H., Köhl, U., Kloess, S., et al. (2015). Selective inhibition of tumor growth by clonal NK cells expressing an ErbB2/HER2-specific chimeric antigen receptor. Mol. Ther. *23*, 330–338. https://doi.org/10.1038/mt.2014.219.

58. Nowakowska, P., Romanski, A., Miller, N., Odendahl, M., Bonig, H., Zhang, C., Seifried, E., Wels, W.S., and Tonn, T. (2018). Clinical grade manufacturing of genetically modified, CAR-expressing NK-92 cells for the treatment of ErbB2-positive malignancies. Cancer Immunol. Immunother. *67*, 25–38. https://doi.org/10.1007/s00262-017-2055-2.

59. Yadav, B., Wennerberg, K., Aittokallio, T., and Tang, J. (2015). Searching for Drug Synergy in Complex Dose-Response Landscapes Using an Interaction Potency Model. Comput. Struct. Biotechnol. J. *13*, 504–513. https://doi.org/10.1016/j.csbj.2015.09.001.